

## Metallic MoS<sub>2</sub> enhances the performance of water-based drilling fluids

F. L. Sun<sup>\*</sup>, Y.L. Song, H. Tang, J. Xu

*West Branch of Sinopec North China Petroleum Engineering Co., Ltd, Zhengzhou, 450000, P.R. China*

In this work, the metal phase MoS<sub>2</sub> was prepared by a simple one-step hydrothermal method, and it was systematically studied by XRD, Raman, SEM, TEM, and other characterization methods. In addition, the tribological behavior of M-MoS<sub>2</sub> in water-based drilling fluids has been extensively studied with a ball-disk tribometer. In addition, the influence of applied load and speed on friction performance is also studied. The experimental results show that the introduction of M-MoS<sub>2</sub> significantly reduces the friction and wear of the material. Among them, M-MoS<sub>2</sub>-5-water-based drilling fluid has the lowest friction coefficient (~0.11).

(Received January 25, 2022; Accepted May 28, 2022)

*Keywords:* MoS<sub>2</sub>, Water-based drilling fluid, Tribological properties

### 1. Introduction

Friction and wear have an inevitable impact on the motorial machinery, resulting in the consumption of energy and damage of equipment, and the prime task of lubricants is to improve energy efficiency and reduce friction and wear of a sliding system[1-5]. Water-based lubricant with outstanding features, including low cost and good environmental compatibility, has been used for numerous areas such as cutting fluid, metal-forming operations, and so on[6-10]. However, its poor lubricity and low viscosity greatly limited the practical application in a wide range of areas[11-14]. Therefore, it is a necessary and promising domain to develop a high-performance additive to improve the tribological performance of the water-based lubricant, and two-dimensional MoS<sub>2</sub> with superb structural features and outstanding lubricating properties can be used as a key class of lubricating additive[15-19].

Nowadays, two-dimensional (2D) layered materials, like graphene and MoS<sub>2</sub>, have gained considerable attention in the search for novel nano-lubricants to reduce friction and wear because of their lamellar structures and easy interlayer sliding ascribed to the weak van der Waals interactions within their molecular layers[20-24]. In the characteristic layered structure of MoS<sub>2</sub>, a Mo atomic layer sandwiched two S atomic layers. And the intralaminar of S–Mo–S layer is strong covalent, while the interlayer of sandwiched structure is weak Van der Waals force, resulting from the decrease in friction coefficient and possessing enhanced reducing-friction and anti-wear properties[25-28]. More importantly, nano-sized MoS<sub>2</sub> shows more excellent tribological

---

\* Corresponding author: fanglongsun@163.com

<https://doi.org/10.15251/CL.2022.195.371>

properties compared to commercial MoS<sub>2</sub>, which can be applied in harsh working environments, e.g. high pressure and high vacuum[29,30].

In this paper, the metal phase MoS<sub>2</sub> nanosheets were synthesized by a simple hydrothermal method. The friction and wear properties of the ball-disk tribometer were compared and studied. In addition, SEM, SMP, and other techniques are used to characterize the morphology of the wear track to understand its friction and wear mechanism. Studies have shown that the tribological properties of M-MoS<sub>2</sub> nanosheets will facilitate the design of new additives to enhance anti-friction and anti-wear properties, and will also expand their practical applications in industry and agriculture.

## **2. Experimental section**

### **2.1. Material**

Molybdenum trioxide was purchased from Shanghai Huayi, thioacetamide was purchased from Shanghai Chemical Reagent Co., Ltd. (Shanghai, China), and urea was purchased from Aladdin. All chemical reagents are of analytical purity and can be used directly without further purification.

### **2.2. Synthesis of metallic MoS<sub>2</sub> nanosheets**

A simple hydrothermal method was used to synthesize metallic molybdenum disulfide. Specifically, first, 36 mg of molybdenum trioxide, 42 mg of thioacetamide, and 360 mg of urea were dissolved in 30 ml of deionized water, and stirring was continued for two hours. Then transfer all the mixture to a 50ml autoclave, keep it at 200°C for 12 hours, and take out the autoclave immediately after keeping it warm for 12 hours to quickly cool down. The resulting black product was washed three times with deionized water and collected. The sample should be stored in deionized water, denoted as M-MoS<sub>2</sub>.

### **2.3. Water-based drilling fluid formulation**

First, adjust the pH of the clean water to 8-10 with caustic soda, then add 3-5% sodium earth powder, add 0.1% CMC after 24 hours of hydration, then stir at high speed for half an hour, then add 0.2-0.3% polypropylene Amide.

### **2.4. Characterization**

XRD (Bruker-AXS), XPS (Thermo Scientific K-Alpha+ system), Raman Microscope (DXR-Thermo Scientific), SEM (JEOL JXA-840A), and TEM analysis (JEOL JEM-2100) are performed to investigate the phase compositions, chemical states, and microstructure of the as-prepared products.

### **2.5. Tribological test**

The anti-friction and anti-wear properties of water-based drilling fluids with different contents of M-MoS<sub>2</sub> were studied using ball-disc friction and wear tester (MS-T3001, China). During the experiment, the speed of the steel ball was kept at 200 rpm, and the load was 3N at room temperature for 30 minutes. In addition, different tribological variables are also studied,

including the concentration of M-MoS<sub>2</sub> additives (1-7 wt %), which are denoted as M-MoS<sub>2</sub>-1, M-MoS<sub>2</sub>-3, M-MoS<sub>2</sub>-5, M-MoS<sub>2</sub>-7. Application load (3-10 N) and speed (100-500rpm). Then, the surface roughness of the worn surface was analyzed by non-contact optical 3D profiler (SMP, NT1100, Veeco WYKO, USA) and SEM analysis (HITACHI S-3400N, Japan).

### 3. Results and discussion

The phase structure and crystallization process of pure M-MoS<sub>2</sub> material were studied using XRD technology, and the results are shown in Figure 1. For pure M-MoS<sub>2</sub>, its characteristic peaks are located at 16.8°, 34.4°, and 57.2°, which can be indexed to the typical (002), (100), and (110) faces of MoS<sub>2</sub> (JCPDS no.37-1492)[31,32]. In addition, Raman spectroscopy was used to detect the presence of MoS<sub>2</sub>, and the results are shown in Figure 2. The MoS<sub>2</sub> has a 2H phase and 1T phase at the same time. Among them, the 145.2 cm<sup>-1</sup>, 233.6 cm<sup>-1</sup>, 334.4 cm<sup>-1</sup> bands are MoS<sub>2</sub> from 1T phase[33,34], and 284.3 cm<sup>-1</sup>, 346.7 cm<sup>-1</sup>, 398.3 cm<sup>-1</sup> band is MoS<sub>2</sub> from the 2H phase[34].

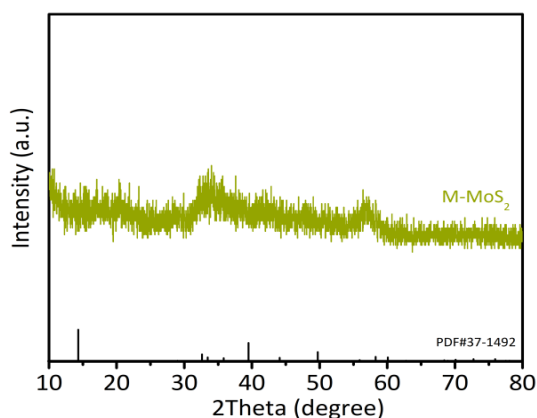


Fig. 1. XRD patterns of M-MoS<sub>2</sub>.

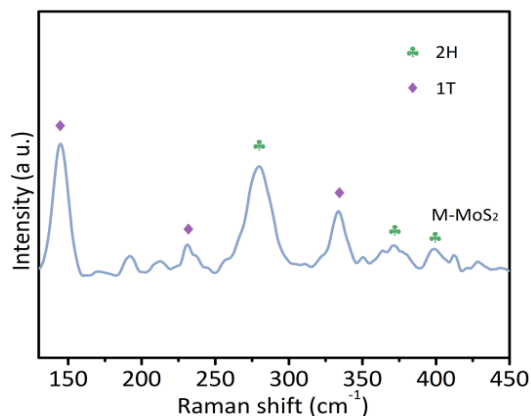


Fig. 2. Raman spectra of M-MoS<sub>2</sub>.

The morphology and structure of flake  $M\text{-MoS}_2$  nanosheets were studied by SEM, as shown in Figure 3.  $\text{MoS}_2$  containing a metallic phase exhibits a typical nanoplate structure (Figure 3a). The TEM image of molybdenum disulfide nanosheets with a size of 100-500 nm is obtained in Fig. 3b. It can also be seen that the molybdenum disulfide nanosheets are disordered, which is consistent with the SEM image observation. In addition, the HRTEM image (Figure 4) shows that the lattice spacing is slightly reduced to 0.574 nm, which can be indexed to the (002) crystal plane of  $\text{MoS}_2$ .

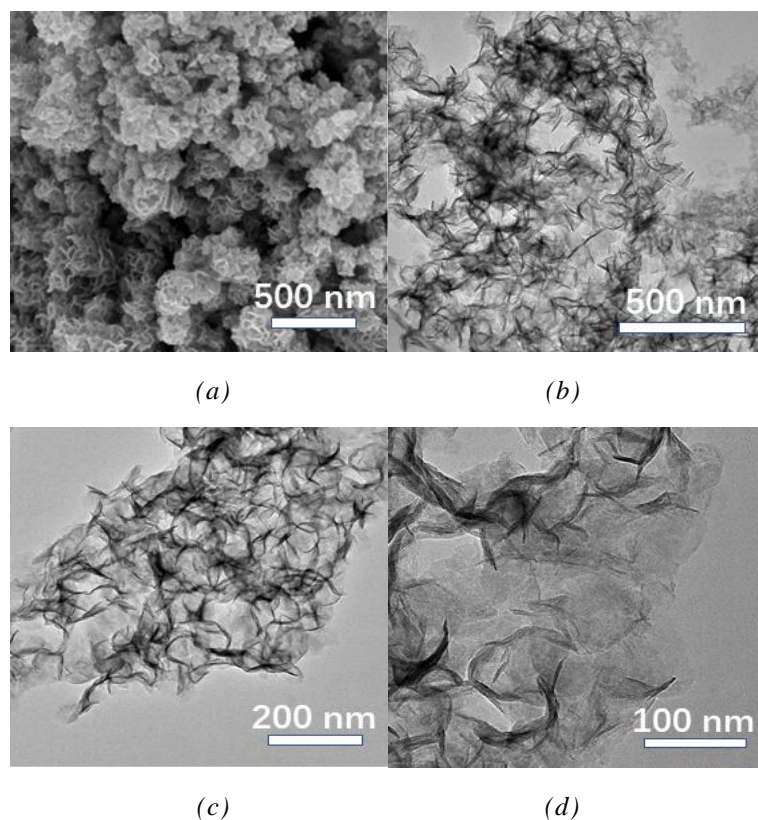


Fig. 3. SEM images of  $M\text{-MoS}_2$ (a)TEM images(b-d) of  $M\text{-MoS}_2$ .

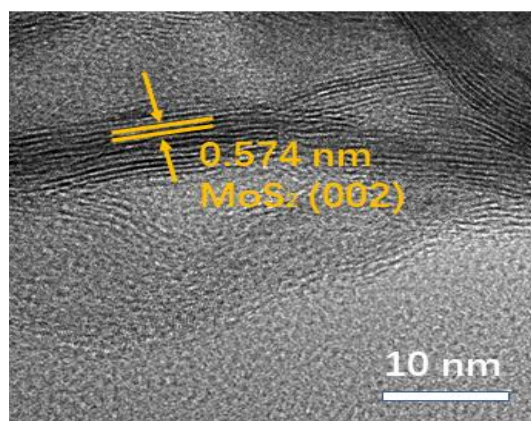


Fig. 4. HRTEM image of  $M\text{-MoS}_2$ .

The Tribological test of synthetic M-MoS<sub>2</sub> and water-based drilling fluid (including M-MoS<sub>2</sub>) is carried out with a ball disc friction meter, as shown in Fig 5a. The average friction coefficient of pure water-based drilling fluid is relatively high, about 0.23. In contrast, the average friction coefficients of water-based drilling fluids of M-MoS<sub>2</sub> and M-MoS<sub>2</sub>-5 gradually decreased to 0.18 and 0.11, respectively. In particular, the optimal addition amount of M-MoS<sub>2</sub> in water-based drilling fluid is 5%, and its average friction coefficient is the lowest compared with other components, which can significantly improve the lubricating effect of water-based drilling fluid (Figure 5b). In addition, the average friction coefficient and time of the M-MoS<sub>2</sub>-5 sample showed a stable change curve (shown in Figure 5b), further indicating that the introduction of M-MoS<sub>2</sub> is a stable friction reduction process. The tribological behavior of M-MoS<sub>2</sub>-5 samples was tested by applying load (3-10N) and rotating speed (100-500 rpm), and comparison experiments were carried out with pure water-based drilling fluid and M-MoS<sub>2</sub> as additives. At a constant speed (200 rpm), the friction curves of water-based drilling fluids with different additives all show similar trends. Under a load of 5N, the average friction coefficient of M-MoS<sub>2</sub>-5 was significantly reduced to 0.11, as shown in Figure 5c. Similarly, as the speed increases, the average friction coefficient curve shows a trend of first decreasing and then increasing, as shown in Figure 5d. The lowest average friction coefficient appeared at 200 rpm, which was mainly due to the addition of M-MoS<sub>2</sub>.

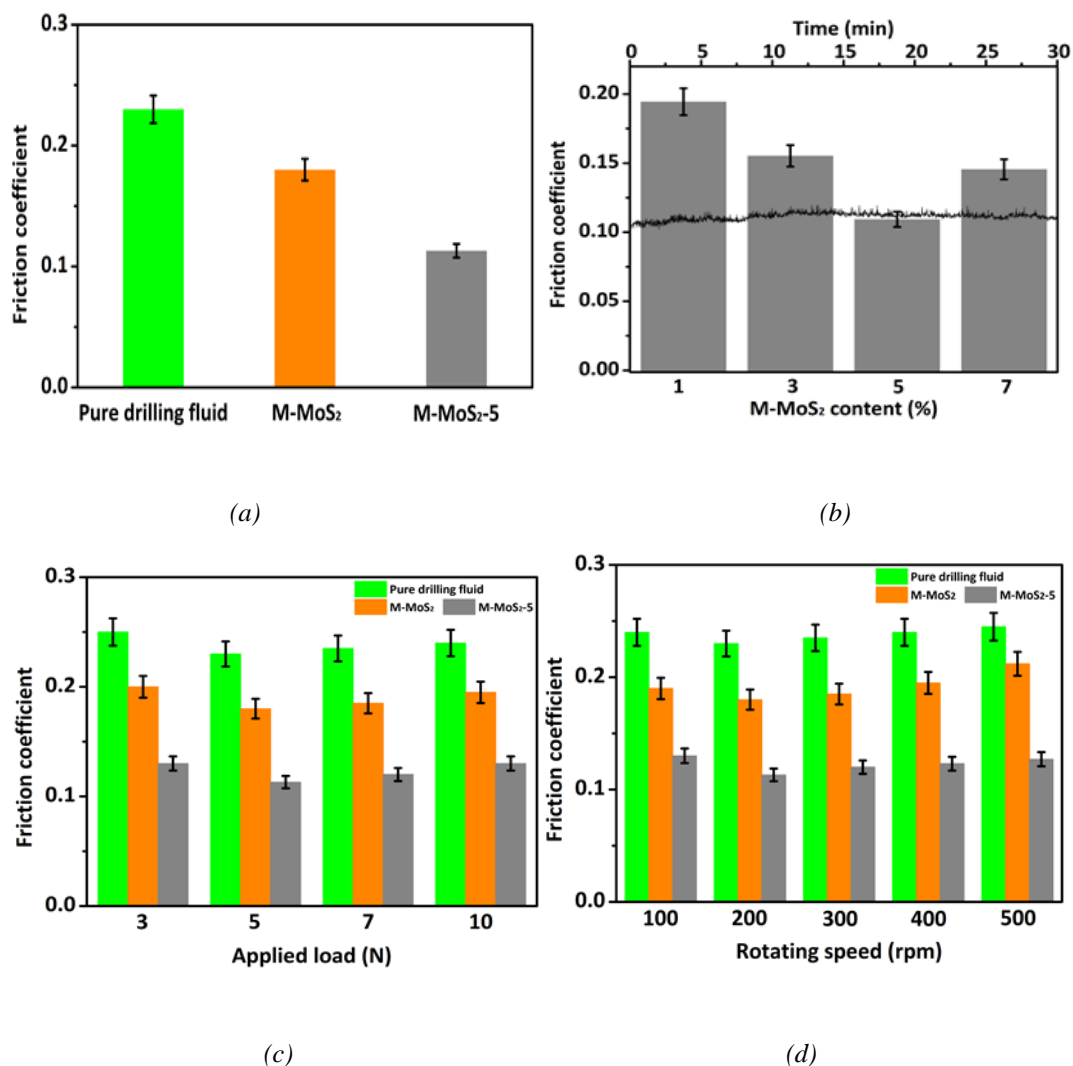


Fig. 5. (a) Coefficient of friction between water-based drilling fluid and additives; (b) Friction coefficient of water-based drilling fluid with different proportions of M-MoS<sub>2</sub> additives; (c) Variation of the average friction coefficient of drilling fluid under different additives and different loads (3-10 N); (d) Variation of the average friction coefficient of drilling fluid at different speeds (100-500 rpm).

To further explore the anti-wear performance and lubrication mechanism of  $M-MoS_2$  in the friction process of water-based drilling fluid, the surface morphology of the worn steel was tested by SEM and SMP analysis methods. From the SEM image (Figure 6a), it can be seen that the surface of the steel disk lubricated by the water-based drilling fluid is severely worn and the wear resistance is relatively poor (Figure 6a). After the introduction of the  $M-MoS_2$  additive, no obvious wear grooves and cracks were observed (Figure 6b). The three-dimensional morphology of the friction interface was accurately detected by SMP technology, as shown in the figure. Similarly, SMP results also show that, compared with pure water-based drilling fluids, the surface morphology of the worn steel lubricated by  $M-MoS_2$  in water-based drilling fluids is relatively smooth. The results show that the wear traces lubricated by water-based drilling fluid are  $3.208\mu m$  and  $178.5\mu m$  (Figure 7a), while the minimum width of wear traces lubricated by water-based drilling fluid containing  $M-MoS_2$  is  $1.203\mu m$  and the depth is  $143.1\mu m$  (Figure 7b). It is also consistent with the wear scar SEM results. The results show that  $M-MoS_2$  material as a lubricant additive has good anti-friction and anti-wear properties.

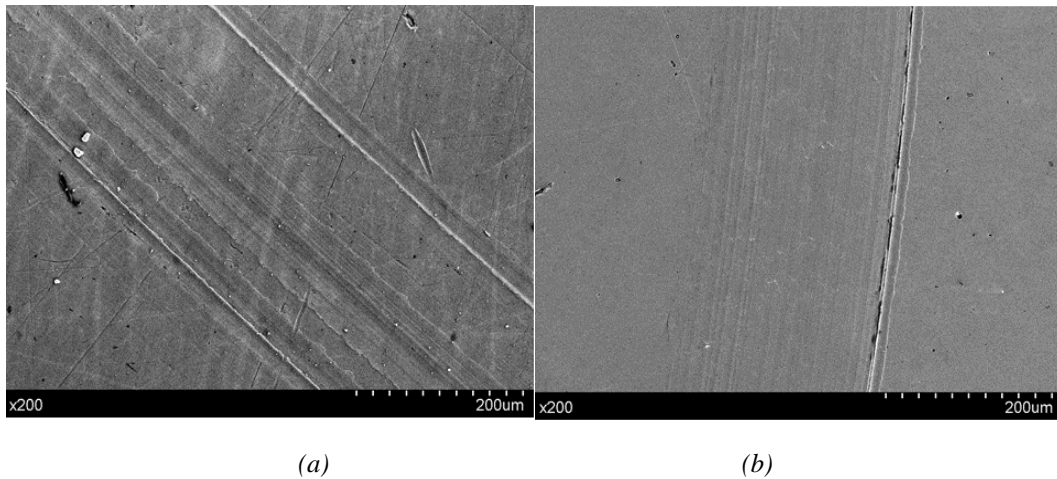
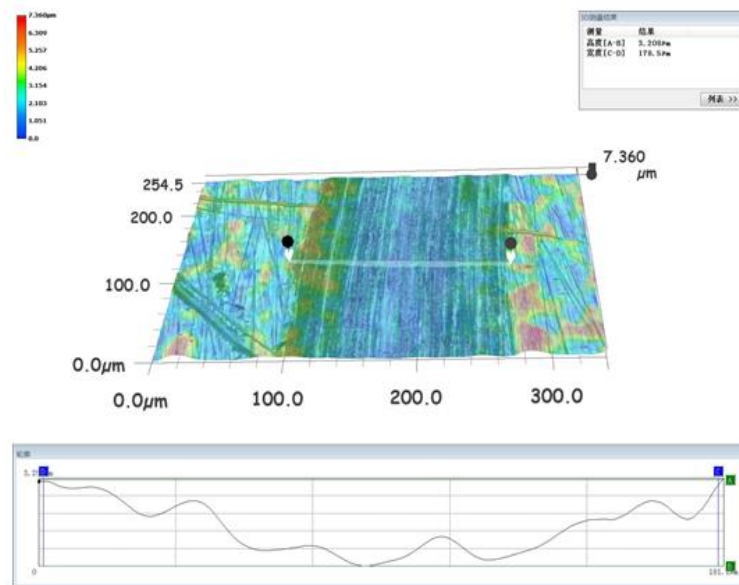
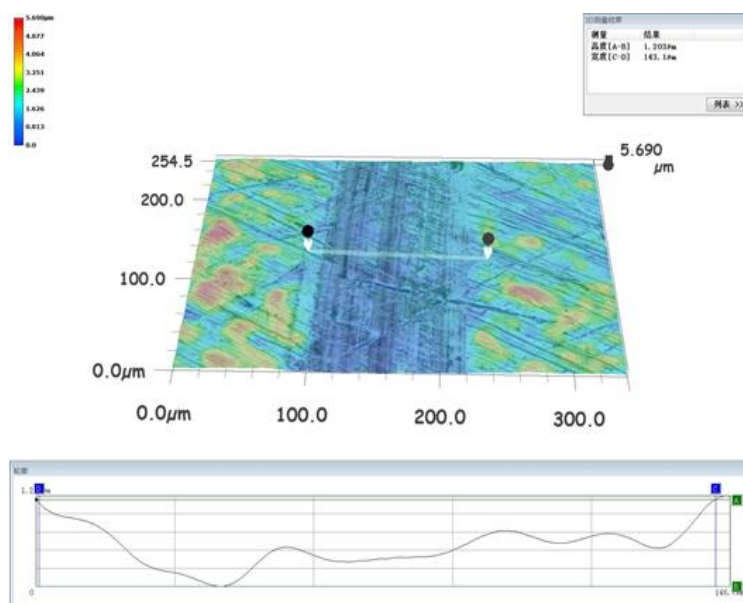


Fig. 6. SEM images of (a) water-based drilling fluid and (b) water-based drilling fluid containing  $M-MoS_2$ .



(a)



(b)

Fig. 7. (a) Water-based drilling fluid and (b) Non-contact three-dimensional image of the worn surface of water-based drilling fluid containing M-MoS<sub>2</sub>.

Based on the above-mentioned tribological experiment results and related analysis of many reports in recent years, a most likely micro-tribological mechanism is proposed. The main reason why the M-MoS<sub>2</sub> material improves the friction and wear performance is its unique microstructure and the formation of friction film. M-MoS<sub>2</sub> adsorbs and deposits on the friction

interface, which hinders the direct contact between the steel disc and the steel ball interface, thereby reducing the friction coefficient and having good anti-wear performance. The SEM analysis of the worn surface is consistent with the conclusion of the wear mechanism.

#### 4. Conclusions

In this paper, a simple one-step hydrothermal method was used to successfully synthesize metallic MoS<sub>2</sub> and use it as a new lubricant additive for water-based drilling fluids. The characterization results show that the MoS<sub>2</sub> nanosheets are more uniformly dispersed. In addition, the tribological behavior of M-MoS<sub>2</sub> in water-based drilling fluids has been extensively studied using a ball-disk tribometer. The results show that the introduction of M-MoS<sub>2</sub> significantly reduces friction and wear in water-based drilling fluids. Among them, M-MoS<sub>2</sub>-5 -water-based drilling fluid has the lowest friction coefficient. The results show that M-MoS<sub>2</sub> exhibits excellent anti-friction and wear properties in water-based drilling fluids, which is conducive to the design of new nano-additives to improve friction and wear properties.

#### References

- [1] K. Holmberg, P. Andersson, et al., *Tribol. Int.* 47 (2012); <https://doi.org/10.1016/j.triboint.2011.11.022>
- [2] A. Tomala, A. Karpinska, et al., *Wear* 269 (2010); <https://doi.org/10.1016/j.wear.2010.08.008>
- [3] E. Serpini, A. Rota, et al. Nanoscale frictional properties of ordered and disordered MoS<sub>2</sub>, *Tribol. Int.* 136 (2019); <https://doi.org/10.1016/j.triboint.2019.03.004>
- [4] K. Ming, H. Minmin, et al. In situ formation of spherical MoS<sub>2</sub> nanoparticles for ultra-low friction. *Nanoscale*, (2018).
- [5] Y. X. Wang, Y. Y. Du, et al., *Colsurfa* 562 (2019); <https://doi.org/10.1016/j.colsurfa.2018.11.047>
- [6] Y. W. Hu, Y. Xin, et al. BLG-RGO: A novel nanoadditive for water-based lubricant. *Tribol. Int.* (2019).
- [7] M. J. Shariatzadeh, D. Grecov, et al., *Cellulose*, (2019); <https://doi.org/10.1007/s10570-019-02398-w>
- [8] Y. Wang, N. Li, et al., *RES CHEM INTERMEDIAT*, (2021). <https://doi.org/10.1007/s11164-020-04356-9>
- [9] H. Wu, J. wei, et al., *J MANUF PROCESS*, (2017); <https://doi.org/10.1016/j.jmapro.2017.03.011>
- [10] Y. Hu, Y. Wang, et al., *Carbon*, (2018); <https://doi.org/10.1016/j.carbon.2018.05.009>
- [11] H. T. Nguyen, K. H. Chung, et al., *Materials*, (2020); <https://doi.org/10.3390/ma13235545>
- [12] Y Hu, Y Wang, C Wang, et al., *Carbon*, (2019); <https://doi.org/10.1016/j.carbon.2019.06.047>
- [13] R. Qiang, L. Hu, et al., *Tribology Letters*, (2019); <https://doi.org/10.1007/s11249-019-1177-4>
- [14] P. Guo, L. Chen, et al., *ACS Appl. Nano Mater*, (2018);

<https://doi.org/10.1021/acsnm.8b01653>

- [15] B. Luan, R. Zhou, et al., APPL PHYS LETT, (2016); <https://doi.org/10.1063/1.4944840>
- [16] W. Chen, C. Tang, et al., Extreme Mech. Lett, (2020);  
<https://doi.org/10.1016/j.eml.2020.100996>
- [17] B. Shi, X. Gan, et al., Nanoscale, (2021); <https://doi.org/10.1039/D1NR04252A>
- [18] R. P. Wu, Z. Liu, et al. Growth of MoS<sub>2</sub> Nanotubes Templated by Halloysite Nanotubes for the Reduction of Friction in Oil. ACS Omega, (2018).
- [19] B. Mba, C. Ms, et al. Friction control by engineering the crystallographic orientation of the lubricating few-layer MoS<sub>2</sub> films. APPL SURF SCI, (2021).
- [20] X. zhong, Z. Y. Tian, et al. Probing the difference in friction performance between graphene and MoS<sub>2</sub> by manipulating the silver nanowires. J. Mater. Sci, (2019).
- [21] H. Ye, Z. J. Ye, et al. Origin of Nanoscale Friction Contrast between Supported Graphene, MoS<sub>2</sub>, and a Graphene/MoS<sub>2</sub> Heterostructure. Nano Letters, (2019).
- [22] Y. Q. Xing, Z. Wu, et al., Surf. Coat. Technol, (2020);  
<https://doi.org/10.1016/j.surfcoat.2020.125396>
- [23] Z. Yang, S. Bhowmick, et al., APPL SURF SCI, (2021);  
<https://doi.org/10.1016/j.apsusc.2021.150270>
- [24] B. Chen, X. Li, et al., Compos. Part A Appl. Sci. Manuf, (2018);  
<https://doi.org/10.1016/j.compositesa.2018.02.039>
- [25] J. Xu, H. Tang, et al., Rsc Advances, (2015); <https://doi.org/10.1039/C5RA06999H>
- [26] X. Li, Z. Cao, et al., APPL SURF SCI, (2006); <https://doi.org/10.1016/j.apsusc.2005.09.068>
- [27] L. Rapoport, V. Leshchinsky, et al., Wear, (2003);  
[https://doi.org/10.1016/S0043-1648\(03\)00044-9](https://doi.org/10.1016/S0043-1648(03)00044-9)
- [28] J. Xu, H. Tang, et al. Facile synthesis and characterization of flower-like MoS<sub>2</sub> microspheres. Chalcogenide Letters, (2014).
- [29] R. Tong, B. Han, et al., MICROGRAVITY SCI TEC, (2021);  
<https://doi.org/10.1007/s12217-021-09896-2>
- [30] L. Kong, K. Huang, et al., Ceramics International, (2021);  
<https://doi.org/10.1016/j.ceramint.2021.04.155>
- [31] A. Mukherji, L. Saikia, et al., Chem. Eng. J., (2019); <https://doi.org/10.1016/j.cej.2019.05.133>
- [32] S. Bolar, S. Shit, et al., Appl. Catal. B, (2019); <https://doi.org/10.1016/j.apcatb.2019.04.028>
- [33] F. Ma, Y. Liang, et al., MATER CHEM PHYS, (2020);  
<https://doi.org/10.1016/j.matchemphys.2020.122642>
- [34] S. Wang, D. Zhang, et al ADV ENERGY MATER, (2018);  
<https://doi.org/10.1002/aenm.201801345>